

The Impact of Plate Imaging Techniques on Flexographic Printed Conductive Traces

Bruce E. Kahn^{a, b, c}, Liam H. O'Hara^{a, b}, and Chip Tonkin^a

^a The Sonoco Institute of Packaging Design and Graphics, Clemson University, Clemson, SC 29634

^b Department of Graphic Communications, Clemson University, Clemson, SC 29634

^c Printed Electronics Consulting, 265 Viennawood Dr., Rochester, NY 14618

E-mail: bkahn@clemson.edu

Howard E. Nelson and William J. Ray

NthDegree Technologies Worldwide Inc., 1320 West Auto Drive, Tempe, AZ 85284

Chris Wargo and Michael Mastropietro

PChem Associates, 3599 Marshall Ln., Suite D, Bensalem, PA 19020

Abstract. There are a number of plate imaging options for flexographic printing. The type of plate used and the way it is processed affect the trace resolution and ink transfer of the conductive material. The authors have recently completed one of, if not the largest research studies ever conducted in printed electronics. Over 45,000 resistances were measured and nearly 1000 three-dimensional optical profiles were obtained, from which a variety of morphological parameters were measured. Many printing variables were examined, including plate material, imaging and plate processing conditions, trace orientation, anilox cell volume, plate type, line and gap width, and orientation. Aqueous, nano-silver inks were printed on both PET and coated paper. The impact of these printing process variables on the conductivity and resulting printed trace width and minimum reverse will be discussed. © 2012 Society for Imaging Science and Technology.

[DOI: 10.2352/J.ImagingSci.Technol.2012.56.4.040507]

INTRODUCTION

Recently, there has been great interest in the use of printing processes for patterning functional materials, and their use in the fabrication of electronic devices. Printing processes offer a number of important characteristics.¹ They are commonly available, and at a wide range of scales, and can scale up easily. They are additive processes, i.e., material is deposited only where desired. The throughput of printing processes can be extremely high—as high as 60 m²/s. Printing processes are normally used in ambient environments, and are compatible with an almost limitless number of materials and substrates. The most common printing processes used for printed electronics are ink-jet,^{2,3} screen,⁴ flexography,^{5,6} and gravure.⁷ Other printing processes have also been used, including pad printing,⁸ soft lithography,^{9,10} offset lithography,^{11–14} thermal transfer,^{15,16} aerosol jet,¹⁷ and direct writing with a pen/stylus.^{18–21} Each of these techniques has its own set of

advantages/disadvantages, and they are frequently combined together^{22–24} for device fabrication.

Flexographic or flexo printing is a high speed roll-to-roll printing process that is widely used in a number of commercial graphics arts applications, particularly in the packaging industry.²⁵ Flexography has also been used for printing functional materials. Flexographic printing is characterized by a flexible and compressible photopolymer image carrier (printing plate) having a raised surface (image area) and a recessed relief (the floor of the plate, non-image area), much like a common rubber stamp. An anilox roll is used to apply ink to the plate. The anilox roll is a cylinder that is uniformly engraved with recessed cells. Commonly, a two-roll system is employed with a metering roll used to transfer ink from the ink pan to the anilox roll, filling the cells with ink. A thin steel doctor blade is used to wipe the excess ink from the roll prior to it coming in contact with the plate. In this study, a chambered doctor blade system was used²⁵, where the ink was contained in a closed chamber integrated with two doctor blades. The printing plate is pushed against the anilox cylinder so that the raised plate surface (image area) comes in contact with the ink within the cells, pulling the ink out of the cells onto the plate surface. An impression roller is used to create a nip with the plate through which the substrate is passed, transferring ink from the plate surface to the substrate. The flexographic printing process has been described in detail.^{1,25}

Flexographic printing offers a number of important advantages over other printing processes. The printing plates are easy to obtain, and relatively inexpensive compared to some other printing processes (i.e., gravure). Since the image carrier (printing plate) is flexible, flexographic printing is conformal, and tolerates substrate morphological variation well. Flexography can be used to print onto almost any type of substrate, and almost any kind of material can be formulated into an ink. The amount of ink that is deposited can be controlled (using the anilox roller) and, fairly uniquely in printed electronics, is independent of the

Received May 18, 2012; accepted for publication Sep. 19, 2012; published online Dec. 6, 2012.

1062-3701/2012/56(4)/040507/08/\$20.00

printed feature dimensions on the printing plate. In most other printing processes used in printed electronics, the amount of ink delivered is strongly correlated to the feature dimensions on the plate. In flexographic printing, the image carrier (printing plate) does not serve as the primary ink metering device, so one is able to adjust the ink thickness without changing the printing plate. Flexographic printing also has some important disadvantages. Printed features can be distorted by plate deformation and ink spreading, and the surface topology of printed features can be nonuniform (thicker in some areas than others).²⁶ While the achievable resolution of flexography has traditionally been thought of as inferior to other printing processes, much progress has been made in this area. The data used in this work include flexographically printed features as small as about 35 μm .²⁷ Even smaller features that have been flexographically printed, as narrow as 15 μm , have recently been reported.²⁸

The experiment was designed to examine various imaging technologies for flexographic platemaking and their impact on printed features. Five different plate types were used, including Kodak NX, Kodak NX DigiCap, a Dupont DPR plate exposed in air and another DPR plate exposed in nitrogen, and an Asahi DEF plate. The plates were selected for this study because of the various technologies employed in their production. These “digital” plates are composed of a UV sensitive photopolymer. The polymerization of the photopolymer is inhibited by the presence of oxygen. Thus, in the presence of air, the polymerization on the surface of the plate takes longer than within the plate material. When making halftones for graphic arts reproductions, this results in dots that have a rounded tip. This was initially regarded as a positive aspect of the plate making, as it provided a natural cutback to the dot size. However, in the graphic arts community there is debate as to whether the round dots offer the same repeatability and crisp print as the flat-topped dots produced in a vacuum. The flat tops, it is argued, do not deform under pressure in the same way as round-top dots do, and as such are presumed to be more consistent and to provide sharper printing. This issue is very relevant for the printing of conductive traces. The traces that are exposed in air have a rounded edge, those exposed in an oxygen free environment have a sharp edge (Figure 1). With the rounded edge, the flat part of the plate is “cut back” slightly, typically of the order of 15 μm per edge, and is narrower than the feature in the design. In an oxygen free exposure, the flat part of the trace is fully as wide as the feature in the mask. In a similar fashion, the line gaps (reverses) are generally wider on a plate exposed in air. As this report will show, these plate features can be used advantageously for printed electronics.

As with halftone dots, printed traces also experience gain as the ink transfers from the plate to the substrate.²⁵ The ink tends to squeeze out to the sides under pressure, creating an image larger than the image carrier on the plate. In halftone printing this is referred to as “dot gain” or “tonal value increase”. Plates exposed in air print thinner traces as they have the natural “cutback” of the oxygen inhibition (*vide*

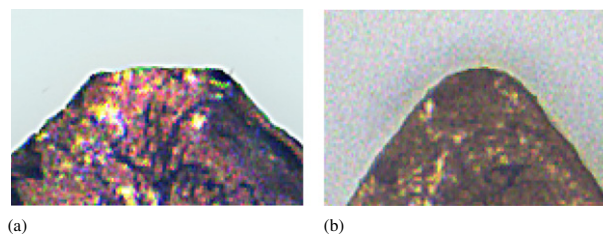


Figure 1. 40 μm (nominal) flexographic plate features exposed in N_2 (a) and air (b).

infra). This issue is anticipated to have greater impact with thinner traces.

We investigated the effect of the presence of air during plate exposure. The Asahi DEF plates are exposed in air and have rounded edges. The Dupont DPR plates allow one to assess the presence of oxygen. One plate was exposed in an ambient atmosphere (Fig. 1(b)) and one was exposed in a modified atmosphere that was flushed with nitrogen to remove air during the exposure (Fig. 1(a)). This nitrogen flush produces sharp edge features instead of the rounded edges of the oxygen inhibited exposures. This comparison is useful because the plate materials are made of the same photopolymer, and possess the same surface energy and hardness. Comparisons between different plate materials will be complicated by factors other than just the trace shape.

Another technology employing sharp edge features is Kodak’s NX plate technology. This technology employs a film layer that is laminated to the plate surface. Thus a film negative is employed, but a vacuum is not required due to the lamination. The lamination also serves as an oxygen barrier, preventing inhibition of the polymerization and allowing dots with sharp edges to be created. Kodak has reported 1:1 pixel reproduction with halftone features as small as 10 μm .²⁹

A variation of this technology is Kodak’s DigiCap NX screening. This provides a textured plate surface rather than a uniformly smooth one as is the case with most flexo plates. The fine pattern of reversed areas is credited with printing smoother solids with less mottling on film substrates.²⁹ There are two possible explanations for this. The fine reverses may create a series of channels to carry more ink, much like the fine cells of the anilox roll. In this way, a greater ink transfer may be possible. It is also possible that under pressure (impression), ink can flow into these channels, reducing the degree to which it is forced out of the sides. Ink mottling is a common print issue when printing on very smooth, non-absorbent substrates like PET, which is favored in printed electronics applications for its smoothness, transparency, and dimensional stability.^{30–33}

We have directly compared the cell patterning of the DigiCap NX screening to the non-patterned NX plate. The issue of sharp versus round edges is directly compared using the Dupont DPR plates exposed in air and nitrogen (oxygen free). A fifth plate, the Asahi DEF, is also exposed in air and provides some balance to the three flat-top technologies (the Kodak plates and DPR in nitrogen). As the different photopolymers employed by the three plate manufacturers

have different surface energies, durometers, and other aspects which can affect ink transfer, the Dupont plates offer the cleanest comparison of round- versus flat-topped features, and the two Kodak NX plates the best comparison of plate cell patterning versus no patterning.

It should be noted that there are a number of other factors convoluted with the plate type (set) which are out of the scope of this initial study. For example, each plate was only made once, and the impression was only set once on the press. There are a variety of factors involved in plate making, mounting, and press operation which warrant further study. One should be a very careful attribution of the differences between sets that were observed in this study to plate type differences alone.

EXPERIMENTAL

Printing equipment

Printing press. The printing was carried out on an OMET Varyflex flexographic printing press. The Omet Varyflex 530 is a 7-station modular multi-platform printing press capable of running substrates up to 0.5 m wide, ranging from 12 to 600 μm thick (including films, foils, and paperboard). This platform approach allows the use of various print modules enabling any combination of flexographic, rotary screen, and gravure printing inline, at speeds up to 200 m/min. The press utilizes automatic registration, with independent servo controllers on each station to ensure a high degree of precision between each printing deck. This is particularly important when using multiple printing processes simultaneously, as the nip pressure (and resulting tension differences) would be extremely difficult to control with a conventional gear train approach. Other typical printing press configurations (such as central impression) may allow a higher degree of registration control, but an inline configuration such as this one provides a much greater degree of flexibility in drying and other processing steps between print stations, so it is well worth the trade-off for most anticipated functional printing applications. In fact, with many likely printed electronics applications, the drying and curing steps will be the limiting factors of the roll-to-roll production speed.²⁷

In this work, a single flexographic printing station was employed. An important component of the flexographic printing system is an engraved ink metering system called an anilox roller, which was fitted with a chambered doctor blade system which allowed a relatively small amount of ink (minimum 375 ml) to be used.

Drying/curing. This press has both hot air and UV curing interstation drying units, for use with aqueous, solvent, and UV curable inks. This allows a great deal of flexibility in the type of ink chemistry that can be used, and because of their installation after each print unit, it allows the ink films to be fully dried prior to the next layer being applied. Traditionally, this is achieved with a high volume hot air blower, but that approach takes up a great deal of space, causes high noise levels, and is not generally as effective at drying ink films as a low volume/high velocity approach.

A Flex Air drying system is installed on this press, which uses an industrial sized (100 hp) air compressor to produce relatively high volumes of dry pressurized air that is piped to the press, heated, and directed at the printed web at high velocities. These air streams are cheaper to heat (and can also be done in a more controlled and safe manner when solvents are involved), and inherently lower humidity. The high velocity air streams disrupt the boundary layer of saturated air that travels with the web, allowing better heat transfer and drying capability. This unique, compact (only 1.4 m high by 2.3 m wide) tunnel dryer is mounted above the press on rails to allow it to be positioned above various stations in the press. In this work the tunnel dryer temperature was 120°C, and the path length was 16.5 m. This resulted in dwell times in the dryer of 33 s at 30.5 m/min. We have also recently shown dwell times of 5 s at 200 m/min.²⁷

The printing in this study was conducted at 30.5 m/min. A corona treatment unit was employed at the unwind of the substrate. The corona treater was set to 400 W and the treated substrate's surface energy measured approximately 44 dyn/cm. The interstation driers and the drying tunnel were set to 120°C (250°F) at 22 psi. The plates were all pre-mounted on sleeves using Lohmann XP 5.0 stickyback.

The substrates used were 2-mil PET Melinex film from Dupont-Teijin and an UltraCast coated paper from SAPPI.

The ink used was PFI-722, a commercially available silver nanoparticle ink, made by PChem associates.

Conductivity measurement

Two-point probe resistance measurements were used for the serpentine line (Figure 2), and reverse (triangle) (Figure 3) measurements. These were performed using a Fluke 287 digital multimeter. Testing of the gap widths (reverses) started with the smallest line widths. After three consecutive opens, the testing for that series was stopped. Each anilox cell volume had 32 reverse targets, for a total 192 reverse measurements per sheet.

Press trials

The plates were created from a single illustrator file that was sent to the various manufacturers to create the plates. The plates were imaged with a series of serpentine traces that were a total of 30 cm in length, or 0.3 m. These traces were imaged vertically (in the press direction) and horizontally (in the cross-press direction) in order to investigate the effect of the trace orientation on ink laydown and conductivity. The total length of each of the lines was 0.3 m. The traces were created with a variety of widths ranging from 10 μm to 100 μm in 10 μm increments, then 150 μm , 200 μm , 300 μm , 400 μm , 500 μm , and 600 μm . The dimensions of these lines correspond to traces ranging from 500 squares (@ 600 μm) to 30,000 squares (@ 10 μm) (nominally).^{34,35}

In these test patterns, the portions of the lines that are perpendicular to the analysis direction are wider (lower resistance) than the portions in the analysis direction (Fig. 2). This design ensures that the resistance measurement is dominated by the resistance in the analysis direction, and

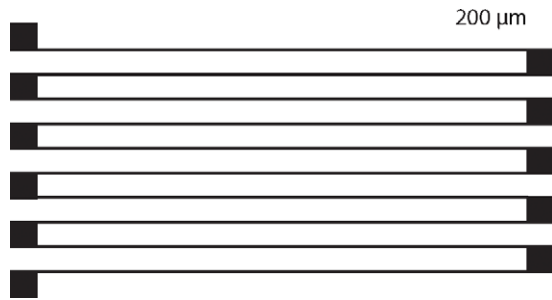


Figure 2. Serpentine line.

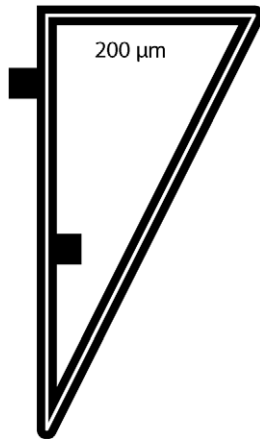


Figure 3. Reverse elements.

helps to differentiate directional effects (anisotropy) on the conductivity.³⁶

In addition, a series of reverse elements were created with line gaps (reverses) ranging from 10 μm to 100 μm in 10 μm increments, and then 100 μm to 500 μm in 20 μm increments, and finally a 550 μm and a 600 μm reverse. The reverses were set in a triangular pattern to test the reverses in the vertical (press direction), horizontal (cross-press direction), and at 26.5° from the vertical angle.³⁷ Fig. 3 illustrates the reverse element design.

The various trace elements were laid out in a 3 × 18-inch area which was then stepped six-out across the press sheet. The six bands were laid out in this way to correspond to the bands of a banded anilox roll. The banded roll is engraved with six different configurations delivering various volumes of ink to the plates. The configurations are specified by the number of engraved cells per linear cm, and the volume of ink delivered, expressed in cm^3/m^2 , or billions of cubic microns per square inch (BCM). The six configurations are shown in Table I. Thus on each plate, there are 192 traces and 192 reverses.

Nine sheets of each press condition were randomly selected for measurement.

RESULTS AND DISCUSSION

Serpentine line conductivity

The resistance values for nine samples (printed sheets) were measured for each press condition. A variety of statistics

Table I. Anilox parameters.

lines/cm	Resolution		Anilox cell volume	
	lines/in	cm^3/m^2	BCM	
472	1200	1.60	1.03	
433	1100	2.37	1.53	
394	1000	2.71	1.75	
354	900	3.44	2.22	
315	800	4.42	2.85	
276	700	5.55	3.58	

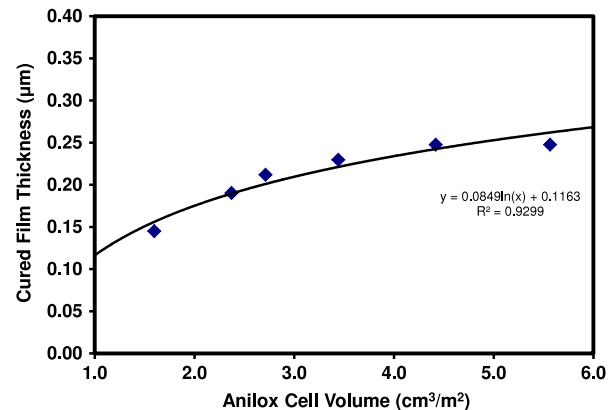


Figure 4. Ink film thickness versus anilox cell volume.

was computed from these data sets, including arithmetic and geometric means, the median, and standard deviations. The median statistic was chosen after comparing the three statistics on a large number of measurements. The median statistic was the least sensitive to outlying measurements, and gave the best representation and visualization for the trends of interest.

Plots of (raw) sheet resistances as a function of (nominal) line width, anilox volume, and orientation are shown in Appendices 1 and 2 (supplementary material). Each of these data sets was fitted to statistical models. Although the statistical modeling was done primarily to assist with visualization, it should be noted that all of these data sets fitted very well. The smallest adjusted r^2 was 0.82. Almost all of the adjusted r^2 values were >0.9 .

A number of trends are immediately apparent. As expected, increasing the anilox cell volume reduces the sheet resistance. This is due to the greater ink film thickness at higher anilox volume (Figure 4), as expected.

There are two other phenomena that can be seen in these graphs, but these must be carefully evaluated because the apparent effects are misleading.

First, there appears to be a dependence of the sheet resistance on the line width. The sheet resistance is lowest at the smallest line widths, and then increases and levels off as the line width increases (Appendix 2, supplementary material). This counterintuitive effect is not real, and is actually caused by the use of nominal line widths to calculate

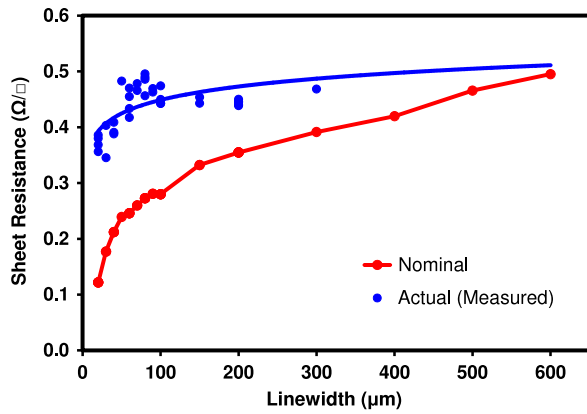


Figure 5. Sheet resistances calculated using nominal and actual (measured) line widths.

the number of squares and sheet resistance. The printed lines are actually wider than the nominal value, and this difference (line gain) has the greatest effect at the lowest line widths. When the actual line widths (measured by optical microscopy or profilometry) are used, the sheet resistances are nearly invariant to line width (Figure 5, Appendix 3 (supplementary material)).

Secondly, the graphs in Appendices 1 and 2 (supplementary material) show that the sheet resistances of the serpentine lines are higher in the horizontal (cross-print, transverse) direction than in the vertical direction. This apparent effect is actually caused by the difference in actual line widths measured in the two directions. The lines obtained in the print direction (vertical, machine) are wider than those perpendicular to the print direction.²⁶ This subtle line width difference almost completely accounts for the differences in sheet resistances between the two directions. This increase in line width could be caused by the fact that in the vertical (print, machine) direction, ink squeezes out on both sides of the trace, whereas the ink squeezes out more on one side than the other in the horizontal (cross-print, transverse) direction. These morphological effects have been studied in detail, and will be the subject of a separate report.²⁶

Since the effect of line gain (the difference between the actual line width and the designed (nominal) line width) is largest at the narrowest line widths, it is possible to minimize this effect by looking at the data from the largest line width studied (600 μm). Fig. 5 also shows that the sheet resistances calculated using the actual line widths level off at approximately the value of the 600 μm (nominal) line width. Therefore, the nominal sheet resistances calculated for the 600 μm lines are a good approximation of the actual sheet resistances. Figure 6 shows the effect of the different plate, substrate, and speed combinations on the sheet resistance using nominal data from the 600 μm line. This technique minimizes the effect of line gain, and compares the data where the variability is smallest.³⁸

It is very apparent from Fig. 6 that the sheet resistance differences are largest at the lowest anilox cell volume. These differences are primarily due to differences in the amount of ink transferred to the plate which controls the

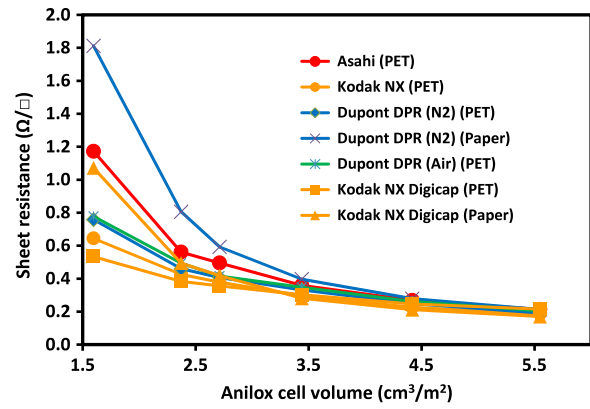


Figure 6. Sheet resistances for different plate and substrate combinations at 600 μm line width.

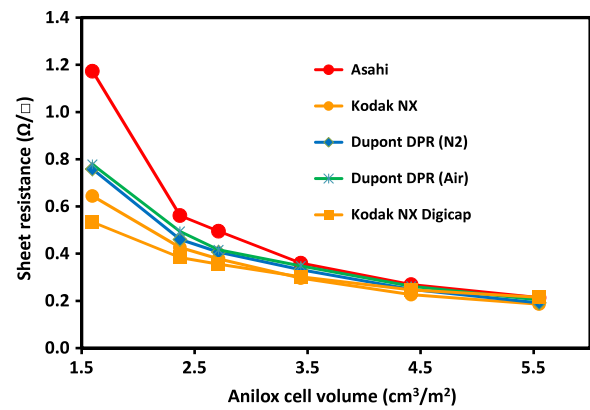


Figure 7. Sheet resistances for different plate materials on PET at 600 μm line width.

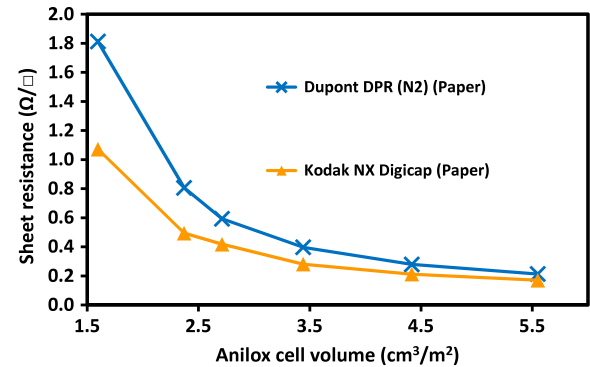


Figure 8. Sheet resistances for different plate materials on Paper at 600 μm line width.

ink film thickness and resulting conductivity. As the anilox cell volume increases, the sheet resistance values tend to converge. This technique can also be used to compare the effect of different plate materials on PET (Figure 7) or paper (Figure 8).

The influence of the substrate on the sheet resistance was investigated for Dupont DPR in N₂, and Kodak DigiCap (Figure 9). For both plate types, the conductivity was better and less sensitive to anilox volume (flatter) on PET than on paper.

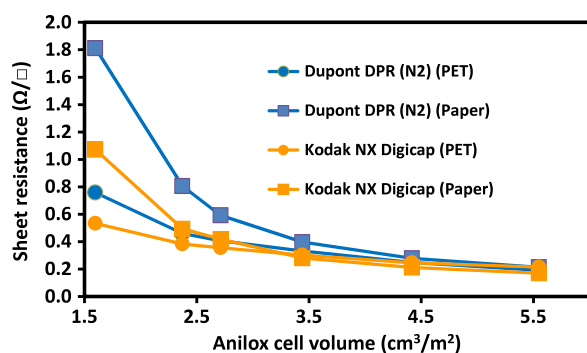


Figure 9. Sheet resistances (600 μm) for Dupont DPR in N_2 and Kodak NX Digicap on PET and paper.

Knowledge of the sheet resistance and the ink film thickness allows one to calculate the resistivity of the printed silver lines. This is the best metric to use, because it takes into account all of the most important conductivity factors—the geometry (number of squares) and the ink film thickness. It also allows the conductivities to be compared with the ultimate limit of conductivity—the bulk resistivity (conductivity) of silver metal ($1.6 \mu\Omega \text{ cm}$). An example of this is shown in Figure 10, where the bulk conductivity of printed lines (as a ratio to that of bulk silver) is plotted as a function of the line width. The shape of this curve is interesting, and fairly typical for the lines investigated in this study. Although the resistivity of the printed lines is fairly flat at about $3.5\text{--}4.5\times$ the resistivity of bulk silver for most of the line width range, there is a significant improvement in conductivity (lower resistivity) at the smallest line widths. This can be understood by examining the height profiles as a function of the line widths (Figure 11). At the smallest line widths, the printed ink is dense and compact. As the line width increases, the ink film spreads out and contains thin spots and low conductivity regions. We believe that this may explain the shape of the resistivity versus line width curve. It is also important to put this result in perspective. It is quite remarkable to think that we can print silver lines, fully cure them inline, and achieve resistivities of only $\sim 3\times$ that of bulk silver! These resistivities are equivalent to or better than the best that have been reported by others.^{39–46} We have also shown that we can print and fully cure silver nanoparticles inline at an unprecedented speed of 200 m/min and throughput of 100 m^2/min .²⁷ At this speed, the silver nanoparticles spend about 5 s curing/sintering, at a very modest (air) temperature of 120°C (the upper processing temperature of heat stabilized PET is $\sim 150^\circ\text{C}$).^{30,33}

Line gaps (reverses)

In addition to requiring fine features and high conductivity, it is also important to be able to place features close to each other without them touching (shorts). As discussed previously, a test pattern to evaluate the minimum achievable line gap was included in the test form. These test patterns were evaluated by measuring the resistances between concentric triangles. A representative example is shown in Figure 12, and

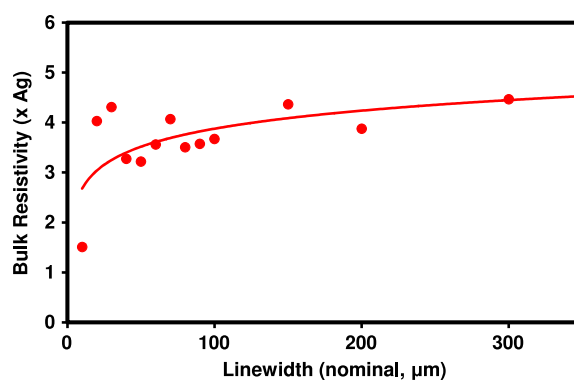


Figure 10. The ratio of printed line resistivity to bulk silver resistivity versus line width (1.75 BCM, Asahi DEF plate).

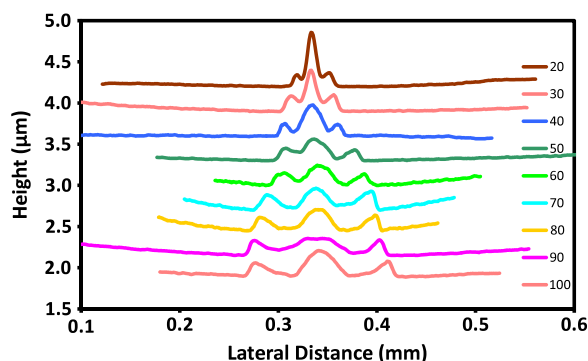


Figure 11. Line width series (Asahi DEF plate, vertical, 1.75 BCM).

the rest of the data are shown in Appendix 4 (supplementary material). Nine printed sheets were measured. The numbers shown in the boxes in Fig. 12 and Appendix 4 are the numbers of sheets (out of nine) for which the given pattern was shorted (i.e., there was an electrical connection between the concentric triangles where there was not designed to be). The smaller the numbers in the boxes (fewer shorts), the better. Where the cells were blank, none of the sheets had electrical shorts. The minimum printable line gap (as a function of anilox cell volume) can be easily seen from this chart. It is apparent that the minimum line gap increases with anilox cell volume (Fig. 12, Appendix 4, supplementary material). This is to be expected. As more ink is deposited, there is a greater chance of shorts between lines, and the minimum line gap increases.

This behavior is summarized in Figure 13. Here, the minimum gap is determined by the line width where there are less than or equal to two shorts out of nine sheets tested. For a given anilox cell volume, the minimum gap range is about 75 μm , depending on the exact conditions (plate, substrate, etc.) used. At $1.6 \text{ cm}^3/\text{m}^2$ (1.03 BCM), the minimum gap was between 30 and 100 μm , whereas at $5.55 \text{ cm}^3/\text{m}^2$ (3.58 BCM), the minimum gap increased to 120–200 μm . Of all of the plates examined, the plates exposed in air (Dupont DPR in air, and Asahi) consistently showed the smallest gap width, likely due to the natural cutback of the oxygen inhibition during polymerization (Fig. 1(b)). This polymerization inhibition makes the raised image (ink

Linewidth (μm) \backslash Anilox Cell Volume	(cm^3/m^2)		1.60	2.37	2.71	3.44	4.42	5.55
	(BCM)		1.03	1.53	1.75	2.22	2.85	3.58
10			9	9	9	9	9	9
20			9	9	9	9	9	9
30			1	9	8	9	9	9
40				9	8	9	9	9
50				1	4	8	9	9
60					2	3	9	9
70			1			2	7	8
80						1	5	7
90			1					6
100							4	8
120							1	2
140							1	1
160								1
180								2
200								2
220								
240								
260								
280								
300								

Figure 12. Gap width versus anilox cell volume for Dupont DPR in air.

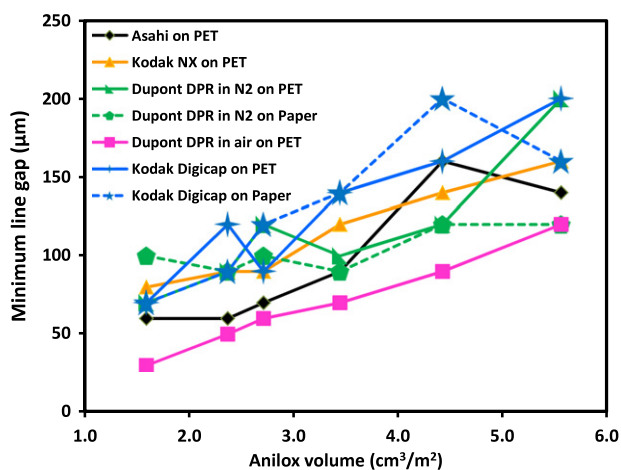


Figure 13. Minimum line gaps versus anilox cell volume.

receiving) areas smaller, the printed lines narrower, and the reverses larger.

CONCLUSIONS

This flexographic printing process capability study investigated a number of factors, including anilox cell volume, plate type and preparation conditions, substrate type, printed feature size and orientation, and line and gap width, using a nanoparticle silver ink. Over 45,000 resistances were measured, and nearly 1000 three-dimensional optical profiles were obtained. We have succeeded in printing and curing silver lines inline on PET having resistivities only $\sim 3\times$ that of bulk silver. As expected, the conductivity of printed serpentine lines increases with anilox cell volume. As the anilox cell volume increases, the differences between other

conditions (plate type, substrate, press speed) diminish. At anilox cell volumes greater than about $3 \text{ cm}^3/\text{m}^2$, the sheet resistances of printed lines for all conditions were very nearly equivalent. The conductivity was better (and less sensitive to anilox cell volume) on PET than on paper. The sheet resistance of serpentine lines (many squares) is nearly invariant to orientation (horizontal or vertical) when actual (measured) line widths are used. The resistivity is slightly smaller (better) at smaller line widths. The minimum line and gap widths were $\leq \sim 40 \mu\text{m}$. The minimum gap width achievable depends upon the anilox cell volume as well as the presence of air during the printing plate fabrication process.

ACKNOWLEDGMENTS

Funding for this project was provided by the FlexTech Alliance (<http://www.flextech.org>) under their agreement with the U.S. Army Research Laboratory.

Supplementary Materials

Supplemental materials available online, <http://ist.publisher.intentaconnect.com/content/ist/jist>.

Conductivity

Appendix 1: R_s (nominal) versus LW, anilox cell volume (BCM) (surface plots).

Appendix 2: R_s (nominal) versus LW, anilox cell volume (BCM) (stacked plots).

Appendix 3: R_s (actual) versus LW, anilox cell volume (BCM).

Line gaps

Appendix 4: Maintainable line gaps as a function of plate type and anilox cell volume.

REFERENCES

- B. E. Kahn, "Organic electronics technology," *Organic Electronics*, 1st edn (Organic Electronics Association, 2006), pp. 19–32.
- T. Shimoda, Y. Matsuki, M. Furusawa, T. Aoki, I. Yudasaka, H. Tanaka, H. Iwasawa, D. Wang, M. Miyasaka, and Y. Takeuchi, "Solution-processed silicon films and transistors," *Nature* **440**, 783–786 (2006).
- H. Sirringhaus, T. Kawase, R. H. Friend, T. Shimoda, M. Inbasekaran, W. Wu, and E. P. Woo, "High-resolution ink-jet printing of all-polymer transistor circuits," *Science* **290**, 2123–2126 (2000).
- D. A. Pardo, G. E. Jabbour, and N. Peyghambarian, "Application of screen printing in the fabrication of organic light-emitting devices," *Adv. Mater.* **12**, 1249–1252 (2000).
- R. Sangoi, C. G. Smith, M. D. Seymour, J. N. Venkataraman, D. M. Clark, M. L. Kleper, and B. E. Kahn, "Printing radio frequency identification (RFID) tag antennas using inks containing silver dispersions," *J. Dispersion Sci. Technol.* **25**, 513–521 (2004).
- T. Maekelae, S. Jussila, H. Kosonen, T. G. Baecklund, H. G. O. Sandberg, and H. Stubb, "Utilizing roll-to-roll techniques for manufacturing source-drain electrodes for all-polymer transistors," *Synth. Met.* **153**, 285–288 (2005).
- T. Makela, S. Jussila, M. Vilkmann, H. Kosonen, and R. Korhonen, "Roll-to-roll method for producing polyaniline patterns on paper," *Synth. Met.* **135–136**, 41–42 (2003).
- A. Knobloch, A. Berndt, and W. Clemens, "Printed polymer transistors," *First International IEEE Conference on Polymers and Adhesives in Microelectronics and Photonics, Incorporating POLY, PEP & Adhesives in Electronics*, 2001, pp. 84–90.
- Y. N. Xia and G. M. Whitesides, "Soft lithography," *Angew. Chem.-Int. Edn.* **37**, 551–575 (1998).
- B. Michel, A. Bernard, A. Bietsch, E. Delamarche, M. Geissler, D. Juncker, H. Kind, J. P. Renault, H. Rothuizen, H. Schmid, P. Schmidt-Winkel, R. Stutz, and H. Wolf, "Printing meets lithography: Soft approaches to high-resolution printing," *IBM J. Res. Dev.* **45**, 697–719 (2001).

- ¹¹ D. Zielke, A. C. Huebler, U. Hahn, N. Brandt, M. Bartzsch, U. Fuegmann, T. Fischer, J. Veres, and S. Ogier, "Polymer-based organic field-effect transistor using offset printed source/drain structures," *Appl. Phys. Lett.* **87**, 123508/1–3 (2005).
- ¹² P. M. Harrey, P. S. A. Evans, B. J. Ramsey, and D. J. Harrison, "Interdigitated capacitors by offset lithography," *J. Electron. Manuf.* **10**, 69–77 (2000).
- ¹³ P. S. A. Evans, B. J. Ramsey, P. M. Harrey, and D. J. Harrison, "Printed analogue filter structures," *Electron. Lett.* **35**, 306–308 (1999).
- ¹⁴ P. S. A. Evans, P. M. Harrey, B. J. Ramsey, and D. J. Harrison, "RF circulator structures via offset lithography," *Electron. Lett.* **35**, 1634–1636 (1999).
- ¹⁵ G. B. Blanchet, Y.-L. Loo, J. A. Rogers, F. Gao, and C. R. Fincher, "Large area, high resolution, dry printing of conducting polymers for organic electronics," *Appl. Phys. Lett.* **82**, 463–465 (2003).
- ¹⁶ G. B. Blanchet, C. R. Fincher, and F. Gao, "Polyaniline nanotube composites: A high-resolution printable conductor," *Appl. Phys. Lett.* **82**, 1290–1292 (2003).
- ¹⁷ B. E. Kahn, "The M3D aerosol jet system, an alternative to ink-jet printing for printed electronics," *Organ. Printed Electron.* **1**, 20–23 (2007).
- ¹⁸ B. Kahn, J. Lewis, H. Liu, P. Martinez, L. Sargeant, and W. Grande, Patterning PEDOT: PSS using a MicroPen. *Abstracts, 32nd Northeast Regional Meeting of the American Chemical Society* (Rochester, NY, 2004) GEN-189.
- ¹⁹ B. E. Kahn, K. Hirschman, W. J. Grande, G. A. Fino, G. Berube, E. A. Groat, and A. Rae, Direct writing of organic devices using continuous liquid dispensing (MicroPen) and metallic particles. *Abstracts, 34th Northeast Regional Meeting of the American Chemical Society* (Binghamton, NY, 2006) NRM-103.
- ²⁰ Y. Xia, B. E. Kahn, G. A. Fino, and W. J. Grande, Patterning organic materials using a micropen. *Abstracts of Papers, 229th ACS National Meeting* (San Diego, CA, 2005) PMSE-162.
- ²¹ Y. Xia, B. E. Kahn, G. A. Fino, and W. J. Grande, Patterning organic materials using a micropen. *PMSE Preprints 2005*, 92, 269.
- ²² A. C. Huebler, F. Doetz, H. Kempa, H. E. Katz, M. Bartzsch, N. Brandt, I. Hennig, U. Fuegmann, S. Vaidyanathan, J. Granstrom, S. Liu, A. Sydorenko, T. Zillger, G. Schmidt, K. Preissler, E. Reichmanis, P. Eckerle, F. Richter, T. Fischer, and U. Hahn, "Ring oscillator fabricated completely by means of mass-printing technologies," *Organ. Electron.* **8**, 480–486 (2007).
- ²³ K. Reuter, H. Kempa, K. D. Deshmukh, H. E. Katz, and A. C. Huebler, "Full-swing organic inverters using a charged perfluorinated electret fabricated by means of mass-printing technologies," *Organ. Electron.* **11**, 95–99 (2010).
- ²⁴ G. C. Schmidt, M. Bellmann, B. Meier, M. Hamsch, K. Reuter, H. Kempa, and A. C. Huebler, "Modified mass printing technique for the realization of source/drain electrodes with high resolution," *Organ. Electron.* **11**, 1683–1687 (2010).
- ²⁵ H. Kipphan, *Handbook of Print Media: Technologies and Production Methods* (Springer-Verlag, 2001).
- ²⁶ B. E. Kahn, L. H. O'Hara, C. E. Tonkin, C. Wargo, M. Mastropietro, H. E. Nelson, and W. J. Ray, Morphological effects of printing process parameters on flexographically printed conductors. 2012, manuscript in preparation.
- ²⁷ B. E. Kahn, L. H. O'Hara, C. Wargo, M. Mastropietro, H. E. Nelson, D. M. Thompson, W. J. Ray, C. Tonkin, and G. Jablonski, The formation of transparent conductive grids using extremely high throughput printing and inline sintering of silver nanoparticles. 2012, submitted for publication.
- ²⁸ M. Mastropietro, Cost Effective, High Resolution Patterning of Conductors Utilizing Silver Nanoparticle Inks with High Speed Traditional Printing Processes. *Flexible Electronics Conference & Exhibition (FlexTech Alliance, Phoenix, AZ, 2012)*.
- ²⁹ Kodak DigiCap NX Screening. Eastman Kodak Company, http://graphics.kodak.com/KodakGCG/uploadedFiles/DigiCapNX_WhitePaper.pdf.
- ³⁰ W. A. MacDonald, "Engineered films for display technologies," *J. Mater. Chem.* **14**, 4–10 (2004).
- ³¹ I. Yakimets, D. MacKerron, P. Giesen, K. J. Kilmartin, M. Goorhuis, E. Meinders, and W. A. MacDonald, "Polymer substrates for flexible electronics: achievements and challenges," *Adv. Mater. Res.* **93–94**, 5–8 (2010).
- ³² W. A. MacDonald, Flexible substrates requirements for organic photovoltaics. *Organic Photovoltaics 2008*, 471–489.
- ³³ W. A. MacDonald, "Structural materials underpinning functional materials: teaching old dogs new tricks," *Polym. Int.* **57**, 672–677 (2008).
- ³⁴ G. Chase, Ohms Per Square What! In ESD Journal; Fowler Associates, Inc., 2011, <http://www.esdjournal.com/techpaper/ohms.htm>.
- ³⁵ C. Wargo, Characterization of conductors for printed electronics. PChem Associates, <http://www.nanopchem.com/pdf/understanding.pdf>.
- ³⁶ R. Sangoi, C. G. Smith, A. Karwa, Y. Xia, F. Sigg, D. M. Clark, W. W. Pope, T. J. Richardson, and B. E. Kahn, "Printing conductive materials using high volume printing processes," *Organic Thin Film Electronics: Materials, Devices, and Applications* (American Chemical Society Miami, FL, 2004).
- ³⁷ R. Sangoi, C. G. Smith, M. D. Seymour, J. N. Venkataraman, D. M. Clark, M. L. Kleper, and B. E. Kahn, "Printing radio frequency identification (RFID) tag antennas using inks containing silver dispersions," *J. Dispersion Sci. Technol.* **25**, 513–521 (2004).
- ³⁸ B. E. Kahn, L. H. O'Hara, C. E. Tonkin, C. Wargo, M. Mastropietro, H. E. Nelson, and W. J. Ray, Flexographic printing process effects on conductivity variability, 2012, manuscript in preparation.
- ³⁹ M. Jung, J. Kim, J. Noh, N. Lim, C. Lim, G. Lee, J. Kim, H. Kang, K. Jung, A. D. Leonard, J. M. Tour, and G. Cho, "All-printed and roll-to-roll-printable 13.56-MHz-operated 1-bit RF tag on plastic foils," *IEEE Trans. Electron Devices* **57**, 571–580 (2010).
- ⁴⁰ I. Reinhold, C. E. Hendriks, R. Eckardt, J. M. Kranenburg, J. Perelaer, R. R. Baumann, and U. S. Schubert, "Argon plasma sintering of inkjet printed silver tracks on polymer substrates," *J. Mater. Chem.* **19**, 3384–3388 (2009).
- ⁴¹ M. Cherrington, T. C. Claypole, D. Deganello, I. Mabbett, T. Watson, and D. Worsley, "Ultrafast near-infrared sintering of a slot-die coated nano-silver conducting ink," *J. Mater. Chem.* **21**, 7562–7564 (2011).
- ⁴² M. Grouchko, A. Kamyshny, C. F. Mihailescu, D. F. Anghel, and S. Magdassi, "Conductive inks with a "built-in" mechanism that enables sintering at room temperature," *ACS Nano* **5**, 3354–3359 (2011).
- ⁴³ J. Perelaer, R. Abbel, S. Wunscher, R. Jani, T. van Lammeren, and S. Schubert Ulrich, "Roll-to-Roll compatible sintering of inkjet printed features by photonic and microwave exposure: from non-conductive ink to 40% bulk silver conductivity in less than 15 seconds," *Adv. Mater.* (2012).
- ⁴⁴ D.-Y. Shin, Y. Lee, and C. H. Kim, "Performance characterization of screen-printed radio-frequency identification antennas with silver nanopaste," *Thin Solid Films* **517**, 6112–6118 (2009).
- ⁴⁵ M. M. Voigt, A. Guite, D.-Y. Chung, R. U. A. Khan, A. J. Campbell, D. D. C. Bradley, F. Meng, J. H. G. Steinke, S. Tierney, I. McCulloch, H. Penxten, L. Lutsen, O. Douheret, J. Manca, U. Brokmann, K. Soennichsen, D. Huelsenberg, W. Bock, C. Barron, N. Blanckaert, S. Springer, J. Grupp, and A. Mosley, "Polymer field-effect transistors fabricated by the sequential gravure printing of polythiophene, two insulator layers, and a metal ink gate," *Adv. Funct. Mater.* **20**, 239–246 (2010).
- ⁴⁶ S.-M. Yi, J.-H. Lee, N.-R. Kim, S. Oh, S. Jang, D. Kim, J. Joung, and Y.-C. Joo, "Improvement of electrical and mechanical properties of ag nanoparticulate films by controlling the oxygen pressure," *J. Electrochem. Soc.* **157**, K254–K259 (2010).